PAPER

Check for updates

Bioactive terpenoids from *Santalum album* derived endophytic fungus *Fusarium* sp. YD-2†

Chong Yan,‡[a] Weiyang Liu,‡[a] Jing Li,[a] Yanlian Deng,[a] Senhua Chen (ID) *[b] and Hongju Liu*[a]

Two new spiromeroterpenoids, namely fusariumin A (**1**) and B (**2**), along with four known terpenoids, asperterpenoid A (**3**), agathic acid (**4**), guignardone N (**5**), and trametenolic acid (**6**), were obtained from the endophytic fungus *Fusarium* sp. YD-2, derived from the twigs of *Santalum album*. Their structures were elucidated by a combination of spectroscopic analyses. The absolute configuration of **1** was determined by single-crystal X-ray diffraction using Cu Kα radiation, and that of **2** was elucidated on the basis of experimental and calculated electronic circular dichroism spectra. Compound **2** exhibited moderate anti-inflammatory activity *in vitro* by inhibiting nitric oxide (NO) production in lipopolysaccharide activated RAW264.7 cells with an IC_{50} value of 50 μM, and compound **3** showed strong anti-inflammatory activity with an IC_{50} value of 1.6 μM. In the antibacterial assay, compound **1** displayed significant activities against *Staphylococcus aureus* and *Pseudomonas aeruginosa* with an MIC value of 6.3 μg mL^{-1}, and compound **3** showed moderate activities against *Salmonella enteritidis* and *Micrococcus luteus* with MIC values of 6.3 and 25.2 μg mL^{-1}, respectively.

Introduction

Santalum album L, called "Tanxiang" in China, is an evergreen and hemi-parasitic tree belonging to the Santalaceae family. The tree was highly valued for its fragrant heartwood (sandalwood), which was used in religious rituals in India and was also used as a medium to carve deities and temples.[1] Sandalwood was also used as a traditional medicine to remedy many ailments[2] and was recorded in Pharmacopoeia of China.[3]

An endophyte is an organism that lives inside a plant. The plants that host endophytes do not show symptoms of disease, at least during the endophytic phase of their life cycle.[4] Endophytes are known to be able to biosynthesize some of the same chemical compounds as their host plant.[5] The metabolites of endophytic fungi, especially in medicinal plants, have been attracting attention as sources of potentially valuable compounds.[6]

As part of our research, a strain of *Fusarium* sp. YD-2 was collected from the twigs of *S. album*. It has been previously reported that endophytic fungi *Fusarium* sp. could produce

School of Pharmacy, Guangdong Medical University, Dongguan, 523808, China. E-mail: liuhj8@mail2.sysu.edu.cn; Fax: +86769-22896560; Tel: +86769-22896599

School of Marine Sciences, Sun Yat-Sen University, Guangzhou 510275, China. E-mail: chensenh@mail.sysu.edu.cn; Tel: +8620-84725459

† Electronic supplementary information (ESI) available: Spectra of all new compounds (¹H NMR, ¹³C NMR, 2D NMR, and HRESIMS). CCDC 1815613. For ESI and crystallographic data in CIF or other electronic format see DOI: 10.1039/c8ra02430h
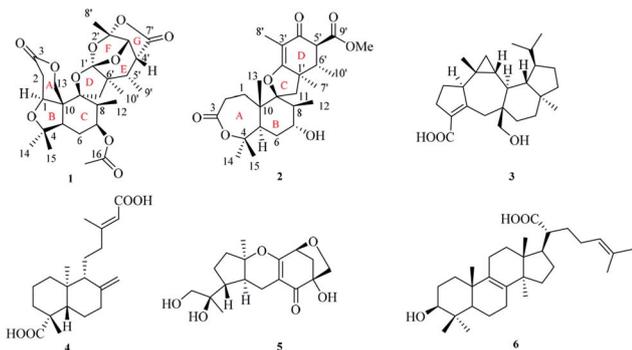
‡ These authors contributed equally to this work.

various bioactive secondary metabolites, such as azaphilone,[7] isocoumarin,[8] isoquinoline,[9] macrolide,[9] cyclic depsipeptide,[10] glycolipid,[11] triterpenoid.[12] Phytochemical analysis of an EtOAc extract of fermentation of the fungus YD-2 led to the identification of two new spiromeroterpenoids (**1** and **2**), along with four known terpenoids (**3–6**). The structures of compounds **1–6** were established by a combination of 1D and 2D NMR data, ECD data analysis, and X-ray diffraction crystallographic data. All isolated compounds were evaluated for anti-inflammatory activities and antibacterial activities. Herein, details of the isolation, structure elucidation, and bioactivities of all isolated compounds are reported.

Results and discussion

The endophytic fungus *Fusarium* sp. YD-2 was cultured on solid rice medium for four weeks. The EtOAc extract of the fermentation was seperated by repeated silica gel chromatography and Sephadex LH-20 column chromatography to afford the compounds **1–6** (Fig. 1).

Fusariumin A (**1**) was obtained as a white solid. The molecular formula determined by HR-ESIMS analysis to be $C_{27}H_{36}O_{10}$, with ten degrees of unsaturation, by observing a quasi-molecular ion at *m/z* 519.2229 [M − H]$^{-}$ (calcd for 519.2236). The ¹H NMR spectrum exhibited signals for seven methyl groups [δ_H 1.02 (d, *J* = 7.5 Hz), H₃-12; 1.28, s, H₃-14; 1.15, s, H₃-15; 2.0, s, H₃-17; 1.74, s, H₃-8′; 1.19 (d, *J* = 7.3 Hz), H₃-9′; 0.90, s, H₃-10′], four methylene groups [δ_H 4.50 (d, *J* = 3.9 Hz), H-1; 2.88 (dd, *J* = 15.9, 4.2 Hz), 2.78 (d, *J* = 15.9, Hz), H-2; 1.65, m, H-6;

Fig. 1 Structures of compounds 1–6.

2.25 (d, $J = 13.8$ Hz), 1.97, (d, $J = 13.8$ Hz), H-11], and seven methine groups [δ_H 4.50 (d, $J = 3.9$ Hz), H-5; 4.85, m, H-7; 2.51, m, H-8; 4.72 (d, $J = 13.0$ Hz), 4.50 (d, $J = 13.0$ Hz), H-13; 4.81 (d, $J = 8.6$ Hz), H-3′; 2.72 (d, $J = 6.3$, 8.6 Hz), H-4′; 2.16, m, H-5′] (Table 1). The ^{13}C NMR and DEPT spectra of 1 revealed the presence of 27 carbon signals, including three carbonyls (δ_C

174.3, 170.4 and 170.1), six quaternary carbons, seven methines, four methylenes, and seven methyls. Three carbonyl carbons accounted for three degrees of unsaturation, remaining seven degrees of unsaturation indicated that the structure of 1 possessed seven rings.

Extensive analysis of 2D NMR, revealed the planar structure of 1 as described below (Fig. 2). The ^{1}H–^{1}H COSY correlations indicated three sequences of CH(1)-CH$_2$(2), CH$_2$(6)-CH(7)-CH(8)-CH$_3$(12), and CH(3′)-CH(4′)-CH(5′)-CH$_3$(9′), as shown by green bold lines in Fig. 2. In the HMBC spectrum, the observed key correlations from H$_3$-14 and H$_3$-15 to C-4 and C-5, from H$_2$-13 to C-1, C-3, C-9, and C-10, from H-1 to C-3 and C-13, from H$_2$-2 to C-3 and C-10, from H$_3$-12 to C-9, from H-17 to C-16 and C-7, from H-7 to C-16 completed the structure of rings A, B, and C (Fig. 2). The HMBC correlations of H-8′ with C-2′ and C-3′, H-3′ with C-1′, C-5′, C-7′ and C-8′, H-4′ with C-6′ and C-7′, H-5′with C-6′ and C-10′, H$_3$-10′ with C-11, C-1′ and C-6′, H$_2$-11 with C-9, C-1′ and C-10′, together with their chemical shift values (δ_C 128.1, C-1′; 107.7, C-2′; 78.7, C-3′) indicated the presence of rings E, F, and G. rings A/B/C and rings E/F/G were connected through a methylene C-11 and an oxygen atom to construct a spiro ring D according to HMBC correlations of H$_2$-11 with C-8, C-9, and C-10. A remaining acetyl group was linked to C-7 (δ_C 72.4) of ring B, supported by the HMBC correlations of H-7 with carbonyl carbon C-16 and H$_3$-17 with C-7.

The relative configuration of 1 was determined by the detailed analysis of NOESY data. The relative configurations of three methyl groups (CH$_3$-12′, CH$_3$-14 and CH$_3$-15) and three methine groups (CH-5, CH-7 and CH-8) in the rings A, B, and C, were identified on the base of key NOESY correlations: H-1/H$_3$-10′, H-6, and H-11α (δ_H 2.25, d, $J = 13.8$), H$_3$-17/H-15 and H$_3$-12, H$_3$-16/H-1. Key NOESY correlations of H-3′ with H-4′ and H$_3$-8′, H-5′ with H-4′ and H-11β (δ_H 1.97, d, $J = 13.8$), H$_3$-10′ with H-11α and H$_3$-9′ indicated that the relative configurations of the rings E, F and G as shown in Fig. 3. Key NOESY correlations of H-8 with H-2β (δ_H 2.78, d, $J = 15.9$), H$_3$-10′ with H-2β and H-11α, H-5 with 11α and H-7 revealed the relative configuration of the two rings system (rings A/B/C and rings E/F/G) as shown in Fig. 3. The absolute configuration of 1 was determined as shown in Fig. 4 by X-ray diffraction analysis using Cu Kα radiation with a Flack parameter of 0.031 (13)[13] (Fig. 3). Fusariumin A (1) was an unusual polycyclic spiromeroterpenoid, whose structure possessed a unique and congested heptacyclic skeleton with 6/5/6/5/6/5/5 system.
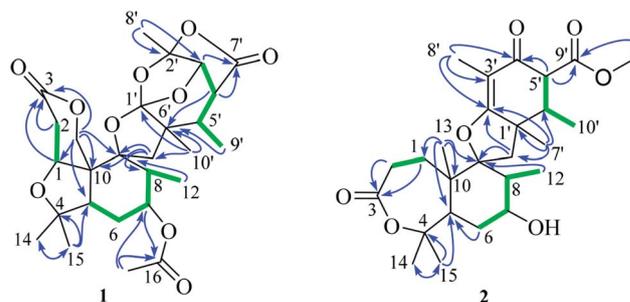
Table 1 ^{1}H and ^{13}C NMR data of compounds 1 and 2

No.	1[a] δ_H (J in Hz)	δ_C	2[b] δ_H (J in Hz)	δ_C
1	4.23, d (3.9)	75.3, CH$_2$	α 1.98, m; β 1.77, m	40.9, CH$_2$
2	α 2.88, dd (15.9, 4.2); β 2.78, d (15.9)	35.5, CH$_2$	2.33, m	32.2, CH$_2$
3		170.1, C		173.3, C
4		80.3, C		85.6, C
5	1.62, dd (11.6, 4.1)	51.2, CH	1.83, m	52.9, CH
6	1.65, m	22.8, CH$_2$	α 2.45, m; β 1.93, m	34.8, CH$_2$
7	4.85, m	72.4, CH	3.91, m	80.5, CH
8	2.51, m	46.0, CH	1.92, m	50.1, CH
9		86.3, C		100.3, C
10		50.0, C		45.5, C
11	α 2.25, d (13.8); β 1.97, d (13.8)	49.9, CH$_2$	α 2.50, m; β 1.87, m	44.5, CH$_2$
12	1.02, d (7.5)	10.8, CH$_3$	0.91, d (7.0)	13.9, CH$_3$
13	α 4.72, d (13.0); β 4.50, d (13.0)	65.5, CH	1.32, s	23.1,CH$_3$
14	1.28, s	30.8, CH$_3$	1.30, s	34.2, CH$_3$
15	1.15, s	21.6, CH$_3$	1.71, s	27.0, CH$_3$
16		170.4, C		
17	2.08, s	21.0, CH$_3$		
1′		128.1, C		44.9, C
2′		107.7, C		186.8, C
3′	4.81, d (8.6)	78.7, CH		106.7, C
4′	2.72, dd (6.3, 8.6)	41.8, CH		195.6, C
5′	2.16, m	39.6, CH	3.32, d (3.4)	59.4, CH
6′		47.4, C	2.52, m	42.8, CH
7′		174.3, C	1.26, s	22.4, CH$_3$
8′	1.74, s	22.2, CH$_3$	1.70, s	8.6, CH$_3$
9′	1.19, d (7.3)	12.2, CH$_3$		173.3, C
10′	0.9, s	19.1, CH$_3$	1.05, d (6.7)	14.7, CH$_3$
11′			3.71, s	52.7, CH$_3$

^{a} ^{1}H (400 MHz) and ^{13}C (100 MHz) NMR data in CDCl$_3$. ^{b} ^{1}H (400 MHz) and ^{13}C (100 MHz) NMR data in MeOH-d_4.

Fig. 2 Key HMBC (blue arrows) and ^{1}H–^{1}H COSY (green bold lines) correlations of 1 and 2.
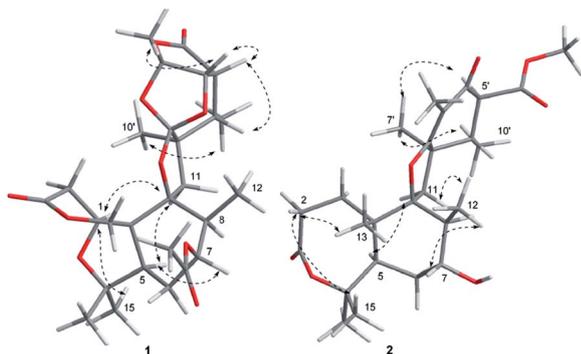
Fig. 3 Key NOESY (dash arrows) correlations of **1** and **2**.

Fusariumin B (**2**) was isolated as a white, amorphous powder. The molecular formula was assigned to be $C_{26}H_{38}O_7$, with eight degrees of unsaturation, based on its HR-ESIMS (m/z 461.2549, calcd for 461.2545). The ^1H NMR spectrum exhibited eight methyl groups, one methoxy group, four methylene groups and five methine groups (Table 1). Three signals (δ_C 195.6, 173.3 and 173.3) in the ^{13}C NMR data revealed the presence of three carbonyl carbons (one ketone and two esters), and two signals (δ_C 186.8, 106.7) revealed one olefin. These units accounted for four degrees of unsaturation, indicating that four rings were present.

The planar structure of **2** was mainly elucidated by 2D NMR (^1H–^1H COSY and HMBC). A seven-membered lactone (ring A) was identified on the base of ^1H–^1H COSY correlation between H_2-1 and H_2-2, and the key HMBC correlations of H_2-1 and H_2-2 with C-3 (δ_C 173.3), H_2-1, H_3-14 and H_3-15 with C-5, H_2-1 with C-9, H_3-14 and H_3-15 with C-4. The ^1H–^1H COSY correlations of H-12, H-8, H-7 with H_2-6 and the HMBC correlations from H_3-12 and H_3-13 to C-9, H-7 to C-5, H_3-13 to C-10 and C-5 indicated the presence of a hexatomic ring (ring B). A cyclohexanone unit (ring D) was established by the HMBC correlations of H-5′ and H-6′ with C-4′ and C-9′, H-6′ and H-7′ with C-1′, H-6′ and H_3-8 with C-4′, H_3-8′ with C-2′ and C-3′, H-7′ with C-2′, H-11′ with C-9′, as well as the ^1H–^1H COSY correlations of H-5′, H-6′ and H-10′. The rings B and D were linked through a methylene C-11 and an oxygen atom to 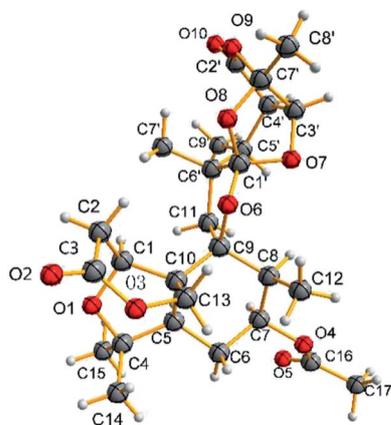construct a tetrahydrofuran with a spiro ring (ring D) based on HMBC correlations of H-7′ with C-1′, H-11 with C-2′, H_2-11 with C-1′, C-2′, C-8 and C-9.

The relative configuration of **2** was established from the analysis of NOESY data (Fig. 3), which was similar to those of asnovolin A.[14] The NOESY correlations of H-1β/H_3-12 and H-6β, H_3-12/H-11β, H-7, H_3-13, H_3-13/H_3-15, H-5, H_3-14/H-1α and H-5 suggested that the three methyl groups (H_3-12, H_3-13, and H_3-14), and H-7 are on the same side in the rings A and B, whereas H_3-15 and H-5 are on the opposite side. The NOESY correlations of H_3-7′/H_3-10′ and H-5′, H_3-10′/H-11α, H-6′/H-11β, indicated that the two methyl groups (H_3-7′ and H_3-10′) and H-5′ are on the same side in the rings C and D.

Compound **2** and asnovolin A showed quite similar ECD spectra (Fig. 5), with a positive cotton effect (CE) at 270 nm and negative cotton effect at 303 nm, indicating that they share the similar absolute configuration. In addition, the absolute configuration of **2** was further assigned by comparison of the experimental and theoretical ECD spectra, which was calculated by a quantum chemical method at the [B3LYP/6-311tg(2d,p)] level. The predicted ECD spectrum of (5R,7R,8S,9S,10S,1′R,5′S,6′S)-**2** was in agreement with that of the experimental one. The absolute configuration of **2** was established as 5R,7R,8S,9S,10S,1′R,5′S,6′S.

Four known compounds, asperterpenoid A (**3**),[15] agathic acid (**4**),[16] guignardone N (**5**),[17] trametenolic acid (**6**)[18] were identified by comparison of their physical and spectroscopic data with those reported in the literature. Asperterpenoid A (**3**), a sesterterpenoid with a new carbon skeleton, was initially isolated from a mangrove endophytic fungus *Aspergillus* sp., which displayed potent inhibitory activity against *Mycobacterium tuberculosis* protein tyrosine phosphatase B (mPTPB).[15] It is firstly reported from the fungus *Fusarium* species herein.

All isolates **1–6** were evaluated for their anti-inflammatory activity *in vitro* by inhibiting nitric oxide (NO) production in lipopolysaccharide (LPS) activated RAW264.7 cells using the Griess assay with indomethacin as the positive control (IC$_{50}$ = 37.5 μM). Compound **2** exhibited moderate anti-inflammatory activity with IC$_{50}$ values of 50.3 μM, while compound **3**
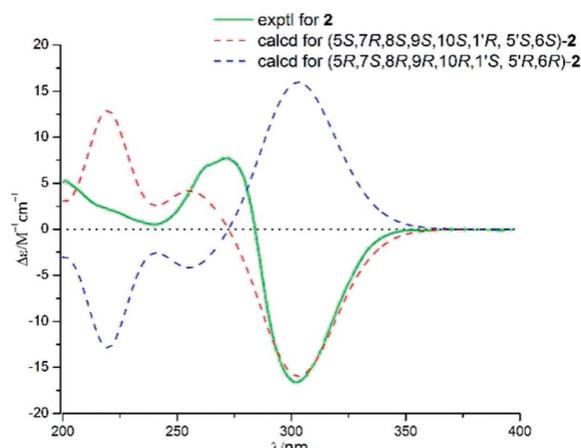

Fig. 4 X-ray crystallographic analysis of compound **1**.

Fig. 5 Experimental and calculated ECD spectra of compound **2** (in MeOH).

showed promising anti-inflammatory activity with IC_{50} value of 1.6 μM (Table 2).

The antibacterial activities of all isolates 1–6 were tested for eight bacteria (*Staphylococcus aureus*, *Staphylococcus albus*, *Bacillus subtilis*, *Bacillus cereus*, *Micrococcus luteus*, *Escherichia coli*, *Pseudomonas aeruginosa*, *Salmonella enteritidis*), using a standard screening protocol.[19] Compound 1 exhibited moderate activities against *S. aureus* and *P. aeruginosa* with MIC value 6.3 μg mL^{-1}. Compounds 3 and 4 showed weak activities against *S. enteritidis* and *M. luteus* (Table 3).

Experimental

General experiment procedures

Optical rotations were measured on an MCP 300 (Anton Paar) polarimeter at 28 °C. Melting points were measured on an X-4 micromelting point apparatus. IR spectrum was recorded on a Nicolet Nexus 670 in KBr discs and UV spectrum was recorded in MeOH solution on a PERSEE TU-1900 spectrophotometer. ECD data were obtained on a Chirascan CD spectrometer (Applied Photophysics). NMR spectra were recorded on a Bruker Avance 400 MHz spectrometer with tetramethylsilane as internal standard. EIMS on a DSQ EI-mass spectrometer (Thermo) and HREIMS data were measured on a MAT9-5XP high-resolution mass spectrometer (Thermo). Sephadex LH-20 and Silica gel (100-200 mesh, 200-300 mesh, Qing dao Marine Chemical Factory, Qingdao, Qingdao, People's Republic of China) were used for column chromatography. Analytical thin layer chromatography (TLC) was performed with GF254 plates (Qingdao Marine Chemical Factory). The reagents in the research process were analytical (Guangzhou chemical reagent factory). Single-crystal data were carried out on an Agilent Gemini Ultra diffractometer (Cu Kα radiation).

Fungal material

The fungus was isolated from twigs of the *Santalum album*, which was collected from Dongguan, Guangdong Province, People's Republic of China, in April 2016. The fungus was obtained using the standard protocol for isolation. Fungal identification was carried out using a molecular biological protocol by DNA amplification and sequencing of the ITS region. The sequence data obtained from the fungal strain which have been deposited at GeneBank with accession no. MH057323. Then A BLAST search result showed that the sequence was the most similar (99%) to the sequence of *Fusarium* sp. (compared to FJ624268.1 KF918593.1).

Fermentation, extraction, and isolation

The fungus was cultured on autoclaved rice solid-substrate medium (100 × 1000 mL Erlenmeyer flasks; each containing 50 g of rice, 50 mL of distilled H_2O) at room temperature under static conditions and daylight for 28 days.

Following incubation, the mycelia and solid rice medium were extracted with EtOAc. The extract was evaporated under reduced pressure to yield 60 g of residue. The residue was then divided into eight fractions (Fr.1–Fr.8) by column chromatography on silica gel, eluting with a gradient of petroleum ether/EtOAc from 1 : 0 to 0 : 1. Fr.3 (200 mg) was applied to silica gel CC, eluting with petroleum ether/EtOAc (v/v, 7 : 3), to obtain compound 6 (4.33 mg, 98%). Fr.4 (5.6 g, 99%) was subsequently separated by Sephadex LH-20 CC eluting with CH_2Cl_2/MeOH (v/v, 1 : 1) to give subfraction Fr.4.1–Fr.4.5. Fr.4.2 was purified on silica gel chromatography (CH_2Cl_2/MeOH v/v, 98 : 2), to yield compounds 1 (3.68 g, 99%) and 2 (5.79 mg, 98%). Fr.4.4 (300 mg) was subjected to repeated Sephadex LH-20 CC (CH_2Cl_2/MeOH v/v, 1 : 1) and silica gel (CH_2Cl_2/MeOH v/v, 98 : 2) to yield compound 3 (3.37 mg, 98%) and compound 4 (3.48 mg, 96%).

Table 2　Anti-inflammatory activity of compounds 1–6 in the LPS-induced RAW 264.7 macrophages

Compounds	IC_{50} (μM)
1	>100
2	50.3
3	1.6
4	>100
5	>100
6	>100
Indometacin[a]	37.5

[a] Indometacin was used as a positive control.

Table 3　Antibacterial activity of compounds 1–6

Compounds	MIC[b] (μg mL^{-1})							
	Staphylococcus aureus	*Staphylococcus albus*	*Bacillus subtilis*	*Bacillus cereus*	*Micrococcus luteus*	*Escherichia coli*	*Pseudomonas aeruginosa*	*Salmonella enteritidis*
1	6.3	>50	>50	>50	>50	>50	6.3	>50
2	>50	>50	>50	>50	>50	>50	>50	>50
3	>50	>50	>50	>50	25.2	>50	>50	6.3
4	>50	>50	>50	12.5	25.4	>50	>50	>50
5	>50	>50	>50	>50	>50	>50	>50	>50
6	>50	>50	>50	>50	>50	>50	>50	>50
Ciprofloxacin[a]	0.25	0.5	0.25	0.5	0.5	0.5	0.5	0.25

[a] Ciprofloxacin was used as positive control. [b] Data was expressed in MIC values.

Fr.5 (208 mg) was also chromatographed on Sephadex LH-20 CC (CH$_2$Cl$_2$/MeOH v/v, 1 : 1) to give subfraction Fr.5.2, which was purified using silica gel (CH$_2$Cl$_2$/MeOH v/v, 97 : 3) to afford **5** (3.65 mg, 96%).

Compound 1. White, amorphous solid; mp 306–308 °C; $[\alpha]_D^{20}$ − 22.2 (c = 0.02, MeOH); UV (MeOH) λ_{max} (log ε) 262 (4.02), 268 (3.81) nm; IR (KBr) ν_{max} 3311, 2917, 2850, 1730, 1639, 1470, 1418, 1393, 1197, 1180, 1103, 1047, 991, 944, 914, 721 cm^{-1}; ^{1}H and ^{13}C NMR, see Table 1; ESIMS m/z 519 [M − H]$^-$; HR-ESIMS m/z 519.2229 [M − H]$^-$, (C$_{27}$H$_{36}$O$_{10}$, calcd for 519.2236).

Compound 2. White, amorphous solid; mp 285–287 °C; $[\alpha]_D^{20}$ − 144.5 (c = 0.02, MeOH); UV (MeOH) λ_{max} (log ε) 270 (4.06) nm; ECD (MeOH) λ_{max} ($\Delta\varepsilon$) 270 (+7.7), 302 (−16.6) nm; IR (KBr) ν_{max} 3363, 2919, 2850, 1737, 1633, 1471, 1392, 1272, 1132 cm^{-1}; ^{1}H and ^{13}C NMR, see Table 1; ESIMS m/z 461 [M − H]$^-$; HR-ESIMS m/z 461.25488 [M − H]$^-$, (C$_{27}$H$_{36}$O$_{10}$, calcd for 461.25448).

X-ray crystallographic analysis of compound 1

Compound **1** was obtained as colourless crystals from CHCl$_3$ using slow evaporation method. Crystal data were obtained at 150 K for **1** on an Agilent Gemini Ultra diffractometer with Cu Kα radiation (λ = 1.54178 Å). The structure was solved by direct methods with SHELXS-97, and all non-hydrogen atoms were refined anisotropically using the least-squares method. All hydrogen atoms were positioned by geometric calculations and difference Fourier overlapping calculations. Crystallographic data for **1** has been deposited at the Cambridge Crystallographic Data Centre.

Crystal data of 1. C$_{27}$H$_{36}$O$_{10}$, M_r = 519.22, orthorhombic, a = 14.11110 (10) Å, b = 11.04240 (10) Å, c = 20.3079 (2) Å, α = 90.00°, β = 94.0100 (10)°, γ = 90.00°, V = 3156.64 (5) Å^3, space group $P2_1$, Z = 2, D_{calcd} = 1.472 mg m^{-3}, μ = 4.271 mm^{-1}, and F (000) = 1460.0. Crystal dimensions: 0.7 × 0.55 × 0.3 mm^3. Independent reflections: 12 189 [R_{int} = 0.0320, R_{sigma} = 0.0357]. The final R_1 values were 0.0605, wR_2 = 0.1718 ($I > 2\sigma(I)$). The goodness of fit on F^2 was 1.043. Flack parameter value was 0.031 (13). CCDC number: 1815613.

Calculation of ECD spectra

Molecular Merck force field (MMFF) and DFT/TD-DFT calculations were carried out with Spartan' 14 software (Wavefunction Inc.) and Gaussian 09 program, respectively. Conformers were generated and optimized using DFT calculations at the B3LYP/6-31G(d) level. Conformers with a Boltzmann distribution over 1% were chosen for ECD calculations in MeOH at the B3LYP/6-311tg(2d,p) level. The IEF-PCM solvent model for MeOH was used. ECD spectra were generated using the program SpecDis 3.0 (University of Würzburg) and Origin Pro 8.5 (Origin Lab, Ltd.) from dipole-length rotational strengths by applying Gaussian band shapes with sigma = 0.30 ev. All calculations were performed by High-Performance Grid Computing Platform of Sun Yat-Sen University.

Antibacterial activity

Metabolites were tested *in vitro* for the antimicrobial activity by the conventional broth dilution assay as described previously.[19] Eight bacterial strains, *Staphylococcus aureus* (ATCC 12598), *Pseudomonas aeruginosa* (ATCC 27853), *Escherichia coli* (ATCC 25922), *Bacillus subtilis* (ATCC 6633), *Staphylococcus albus* (ATCC 8032), *Bacillus cereus* (ATCC 14579), *Micrococcus luteus* (ATCC 10240), and *Salmonella enteritidis* (ATCC 13076) were used.

Cell viability assay and anti-inflammatory activity

Cell viability was measured using the conventional MTT assay.[20] RAW 264.7 cells were seeded in 96-well plates at a density of 1.5 × 10^5 cells per mL. After 12 h, the cells were treated with LPS (1 μg mL^{-1}) and samples, followed by additional incubation for 24 h at 37 °C. MTT stock solution (2 mg mL^{-1}) was added to wells for a total reaction volume of 110 μL. After 4 h incubation, the supernatants were aspirated. The formazan crystals in each well were dissolved in 50 μL of DMSO, and the absorbance was measured using a microplate reader (ThermoMax, Sunnyvale, CA, USA) at the wavelength of 490 nm. Relative cell viability was evaluated based on the quantity of MTT converted to the insoluble formazan salt. The optical density of formazan generated in the control cells represented 100% viability. The data were expressed as mean percentages of the viable cells compared to the respective control.

After pre-incubation of RAW 264.7 cells (1.5 × 10^5 cells per mL) with LPS (1 μg mL^{-1}) and samples at 37 °C for 24 h, the quantity of nitrite accumulated in the culture medium was measured as an indicator of NO production.[21] Briefly, 50 μL of cell culture medium were mixed with 100 μL Griess reagent, and incubated at room temperature for 10 min, and absorbance was measured at 540 nm in a microplate reader (ThermoMax, Sunnyvale, CA, USA). Fresh culture medium was used as the blank in all determinations.

Conclusions

In summary, six fungal metabolites (**1–6**), including two new spiromeroterpenoids, fusariumin A (**1**) and B (**2**), were isolated from the *Santalum album* derived endophytic fungus *Fusarium* sp. YD-2 in rice solid-substrate fermentation. Fusariumin A (**1**) was an unusual polycyclic spiromeroterpenoid, whose structure possessed a unique and congested heptacyclic skeleton with 6/5/6/5/6/5/5 system. Compound **1** exhibited selective activities against *Staphylococcus aureus* and *Pseudomonas aeruginosa*, and compound **3** exhibited moderate activities against *Salmonella enteritidis* and *Micrococcus luteus*. The potent anti-inflammatory activity of compound **3**, suggested that **3** would be a promising lead compound for the development of inflammatory inhibitor agent.

Conflicts of interest

There are no conflicts to declare.

Acknowledgements

Notes and references

1 G. A. Burdock and I. G. Carabin, *Food Chem. Toxicol.*, 2008, **46**, 421–432.

2 J. A. Duke, *CRC Handbook of Medicinal Herbs*, Boca Raton, CRC Press. Inc., 1985, pp. 426–427.

3 Chinese Pharmacopoeia Commission, *The Pharmacopoeia of Chinese People's Republic*, ed. Y. Li, The Chemical Industry Publishing House, Beijing, China, 2015, vol. 1, pp. 380–381.

4 D. Wilson, *Oikos*, 1995, **73**, 274–276.

5 H. W. Zhang, Y. C. Song and R. X. Tan, *Nat. Prod. Rep.*, 2006, **23**, 753–771.

6 P. Golinska, M. Wypij, G. Agarkar, D. Rathod, H. Dahm and M. Rai, *Antonie van Leeuwenhoek*, 2015, **108**, 267–289.

7 S. Yang, J. Gao, H. Laatsch, J. Tian and G. Pescitelli, *Chirality*, 2012, **24**, 621–627.

8 S. Yang, J. Gao, Q. Zhang and H. Laatsch, *Bioorg. Med. Chem. Lett.*, 2011, **21**, 1887–1889.

9 S. Yang, J. Xiao, H. Laatsch, J. Holstein, B. Dittrich, Q. Zhang and J. Gao, *Tetrahedron Lett.*, 2012, **53**, 6372–6375.

10 A. R. Ola, D. Thomy, D. Lai, H. Brötzoesterhelt and P. Proksch, *J. Nat. Prod.*, 2013, **76**, 2094–2099.

11 S. Yang, H. Wang, J. Gao, Q. Zhang, H. Laatsch and Y. Kuang, *Org. Biomol. Chem.*, 2012, **10**, 819–824.

12 S. R. Ibrahim, H. M. Abdallah, G. A. Mohamed and S. A. Ross, *Fitoterapia*, 2016, **112**, 161–167.

13 H. D. Flack, *Acta Crystallogr., Sect. A: Found. Crystallogr.*, 1983, **39**, 876–881.

14 K. Ishikawa, F. Sato, T. Itabashi, H. Wachi, H. Takeda, D. Wakana, T. Yaguchi, K. I. Kawai and T. Hosoe, *J. Nat. Prod.*, 2016, **79**, 2167–2174.

15 X. Huang, H. Huang, H. Li, X. Sun, H. Huang, Y. Lu, Y. Lin, Y. Long and Z. She, *Org. Lett.*, 2013, **15**, 721–723.

16 A. B Souza, M. G. M. Souza, M. A. Moreira, M. R. Moreira, N. A. J. C. Furtado, C. H. G. Martins, J. K. Bastos, R. A. Santos, V. C. G. Heleno, S. R. Ambrosio and R. C. S. veneziani, *Molecules*, 2011, **16**, 9611–9619.

17 T. Li, M. Yang, X. Wang, Y. Wang and L. Kong, *J. Nat. Prod.*, 2015, **78**, 2511–2520.

18 K. Yoshikawa, K. Matsumoto and S. Arihara, *J. Nat. Prod.*, 2016, **62**, 543–545.

19 S. Chen, Y. Liu, Z. Liu, R. Cai, Y. Lu, X. Huang and Z. She, *RSC Adv.*, 2016, **6**, 26412–26420.

20 J. B. S. Anouhe, A. A. Adima, F. B. Niamké, D. Stien, B. K. Amian, P. A. Blandinières, D. Virieux, J. L. Pirat, S. Kati-Coulibaly and N. Amusant, *Phytochem. Lett.*, 2015, **12**, 158–163.

21 K. S. Kim, X. Cui, D. S. Lee, W. Ko, J. H. Sohn, J. H. Yim, R. B. An, Y. C. Kim and H. Oh, *Int. J. Mol. Sci.*, 2014, **15**, 23749–23765.